

Development of a Device for Measuring the Sensitivity Area of coil Arrays for Magnetic Induction Measurements

Axel Cordes, Susana Aguiar Santos and Steffen Leonhardt

Abstract— Combining single coils to form a coil array provide advantages for magnetic induction measurements of breathing or heart activity. The main goal for such combination could be a coil configuration which makes the whole measurement system less sensitive for moving artifacts of the patient due to the capability of using many coils for signal acquisition. Such setup could be designed and tested with FEM software. But in most cases, the technical realization differs from theoretical, for instance due to cable effects or the presence of amplifiers attached very close to the coils. Thus, a measurement system for detecting the sensitive area of real arrays is required. In this article, such a device is presented. Based on a crane construction, it is well suited for testing arrays which are built for an integration under a bed or within an incubator for vital parameter monitoring. We will describe the construction as well as first example measurements of a test array.

I. INTRODUCTION

Magnetic Induction Measurements provide an option for wireless detection of breathing and heart activity of a patient. Therefore, this technique is well suited for monitoring patients with third degree burns or neonates inside an incubator where cables stress the patients or lead to skin irritations. Since the measurement technique is sensitive to vital parameters, as well as to moving artifacts of the patient, some kind of mechanism reducing these artifacts is required. One possible approach is to use additional measurement channels, which provides the detection of vital parameter at multiple positions on the bed and hence provides redundancy. Each measurement channel requires one coil under the bed. A combination of several coils is called "coil array". Design and functionality of the array could be simulated with FEM during the construction process. In some cases, the results differ from the theoretical design. Reasons for that could be cables or amplifiers which are connected very close to the coils but can not be simulated with FEM. Fabrication tolerances might also lead in suboptimal conditions and may disturb the effective sensitivity area of the coil array. For testing and optimizing coil arrays with the focus on the sensitivity area, a measurement device is required.

II. BASICS

Magnetic impedance measurements are based on magnetic fields (see [1] for introduction in detail). Mathematically, the measurement technique is based on Maxwell laws (see (1) to (3)), where H and E stands for the magnetic and the electrical fields, J is the current density and B stands

for the magnetic flux density. D describes the electric displacement, σ is the conductivity.

$$\text{rot}\mathbf{H} = \mathbf{J} + \frac{\partial\mathbf{D}}{\partial t} \quad (1)$$

$$\text{rot}\mathbf{E} = -\frac{\partial\mathbf{B}}{\partial t} \quad (2)$$

$$\mathbf{J} = \sigma\mathbf{E} \quad (3)$$

An excitation magnetic field induces a small voltage inside the thorax. This voltage will drive a small eddy current. The magnitude and phase of the current are influenced by the local tissue impedance. However, the local impedance is affected by breathing and heart activity which results in local and time dependent eddy currents. By measuring the magnitude and phase of the reinduced fields, detection of heart activity and breathing is feasible.

The reinduced fields are measured through a single or a combination of coils. Thus, a magnetic field component orthogonal to the coil area is measured (Figure 1 -the vector c). However, this is true for ideal coils. In technical realizations

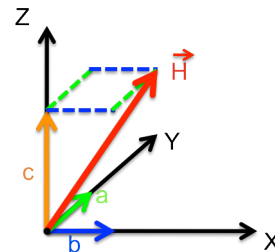


Fig. 1. Vector coordinates

parts of the a and b components would be detected as well. Based of the operation theory described above, some requirements for the measurement device could be defined:

- Avoid usage of metal: Each moving electrical conductive part influences the measurements.
- Separate measurements for each vector coordinate: reconstruction of the vector H (see Figure 1).
- Realize modular construction: The testing area and height should be easy to modify for adapting the setup to special coil configurations
- Be able to scan flat arrays of coils.

III. IMPLEMENTATION

According to these requirements, the device was built as a XY-Plotter based on plastic parts. To make sure that the XY-Plotter can be adapted to large or small arrays we constructed

A. Cordes, S. A. Santos and S. Leonhardt are with the Philips Chair for of Medical Information Technology, RWTH Aachen University, Aachen, Germany cordes@hia.rwth-aachen.de

the system on basis of fishertechnik[®] hardware (other plastic toy systems like LEGO[®] could be used as well). However, we are not the first one who are using such a device in magnetic induction measurements. Other groups ([2], [3] for instance) have been using plotter devices for magnetic induction imaging to scan probes. And thus, the measurement and excitation coils are moved over an area of probes. In this article, we move an phantom over a complex coil array and characterize it. A photo of our plotter is presented in Figure 2. Since the system is based on plastic parts, the

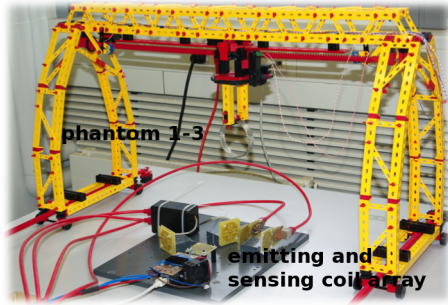


Fig. 2. Photo of the XY-Plotter over the used test coil array

stability is lower compared to a system based on carbon fiber for instance. But it is more flexible, cheaper and the construction is robust enough for the measurement setup. The plotter has an usable height of 360 mm and a width of 412 mm. However, as explained above, these dimensions could be modified with common fishertechnik[®] pieces. For the generation of reinduced fields with the orientation in x-, y- and z-axis a metal ring is moved over the array. The three different orientations of the phantoms (fix1 to fix3) are presented in Figure 3. Because of the high conductivity of the metal ring, the eddy currents, induced in the phantom, are higher than the expected ones in biological tissue. However, this influences only the magnitude of the measurement data and not the local distribution in general. The vector names

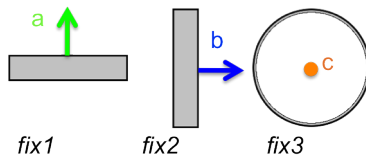


Fig. 3. Three different phantom orientations for x,y and z-component analysis (view from top)

correspond to the names in Figure 1. As shown, the vector H is a summation of the measurements for each phantom 1-3. Photos of the phantom fix 1,2 and fix 3 are shown in Figure 4. The orientation of the reinduced magnetic vectors are the result of induced eddy currents in the phantoms. The used metal ring for the phantoms has a diameter of 70 mm, a width of 15 mm and a thickness of 1.5 mm. They are moved over the array under test in lines with the same length (412mm). The data points between these scan lines are interpolated after the measurements. An interface board was



Fig. 4. Photos of the phantoms (left: fix 1,2, right: fix 3).

developed to control the plotter. On this board, a TI MSP430 microcontroller in combination with L293D H-bridges are used to control the crane motors and USB is used to contact the board to LabView[®]. This program defines motor speed and direction to move the phantom over the coil array. The radio signal is generated and measured with a modified version of the Multi-Channel-Simultaneous-Magnetic-Impedance-Tomography-System (MUSIMITOS, [4]) which enables measurements up to 30 MHz, as well as data recording. Visualization and signal analysis have been performed using Matlab[®].

IV. MEASUREMENTS

A. Setup

For the device validation, we used a test coil array (photo in Figure 2 and top-view with names in Figure 5). All measurement coils are in a orthogonal position to the

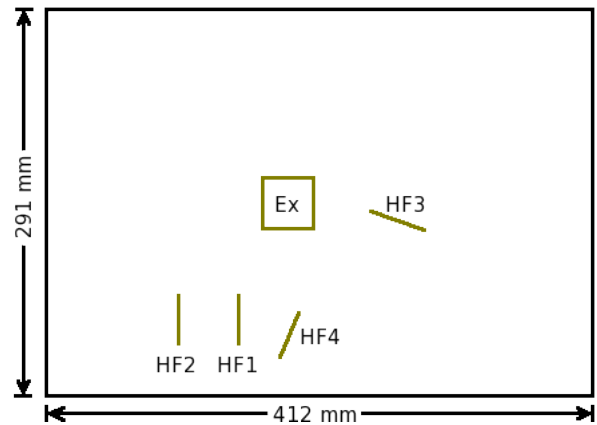


Fig. 5. Names of the coils used for the results. Excitation Coil (EX) and Measurement Coils (HFx)

excitation field. With this setup, only the reinduced fields of the phantom are measured and not the excitation field itself (ideally). With the presented coil configuration, the coils HF1 and HF2 should only be sensitive for reinduced fields generated through phantom 2 and not for 1 or 3 due to the orientation of the fields (orthogonal fields). On the array, HF3 and HF4 should be sensitive for parts of the fields of phantom 1 and 2. All measurement coils are made of PCB with a diameter of 36 mm (HF1, HF3, HF4: 8 windings, HF2: 4 windings). The excitation coil has 2

windings with the same diameter as the measurement coils and the excitation current was 400 mA. As described above, we used a modified version of MUSIMITOS to generate an excitation signal of 10 MHz. The signals of all measurement coils are recorded and demodulated simultaneously. For the measurements, all three phantoms were used separately. The metal ring was placed 163 mm (center of phantom 1 and 2) and 177 mm (phantom 3) above the excitation coils (approx. to the measurement coils) and moved over the complete useable area in x- and y-direction.

B. Results

For each of the three phantoms, three measurements were performed. The presented results only show the mean values minus a base measurement with no phantom. For the characterization of the full array, we analyzed each measurement channel separately. In the Figures, the position of the excitation coil (rectangle) and of the used measurement coil (line) are marked.

Figures 6 and 7 show the measurements recorded on HF1 with the phantoms 1 and 2. The amplitude of the values represent the magnitude of the measurement signal. As

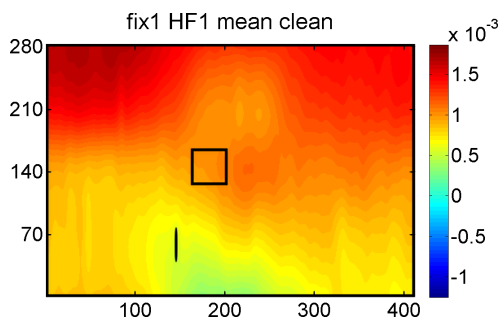


Fig. 6. Test with phantom 1 recorded at HF1 (x-y-axis: dimensions measurement area, amplitude measurement signale (digital unit))

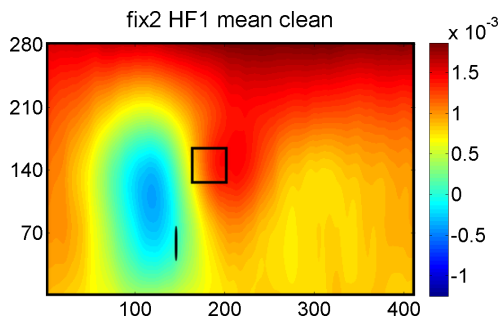


Fig. 7. Data of test with phantom 2 at HF1 (x-y-axis: dimensions measurement area, amplitude measurement signale (digital unit))

expected, the coil is only sensitive for reinduced fields generated by the phantom 2. No significant change in the measurement values could be detected. If there was an influence of the phantom, an area of high signal magnitude would be present in the plot. This could be also measured with HF2. The comparison of Figure 7 with the results for HF2 in Figure 8 illustrate that the maximum sensitivity point

(concentrated area of high magnitude of the measurement signal) of HF2 is more to the left than for HF1. This is directly coupled to the position of both measurement coils and thus fits perfectly to the expected behavior of the coil configuration. The differences in the amplitude's maximum

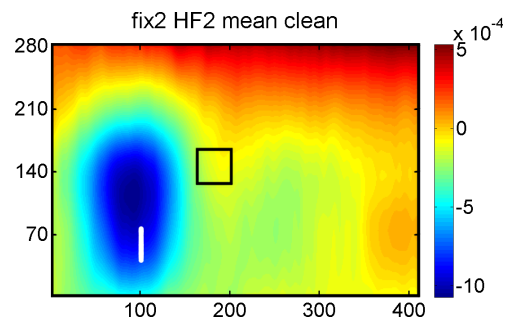


Fig. 8. Data of test with phantom 2 recorded with HF2 (x-y-axis: dimensions measurement area, amplitude measurement signal (digital unit))

is the result of less windings in measurement coil HF2. The plots for HF3 (plotted in Figure 9 and 10) and HF4 (shown in Figure 11 and 12) for the phantoms 1 and 2 show, that both coils are sensitive to fields in x- and y-direction. The effective H-vector in xy-orientation is also between the x- and y-axis.

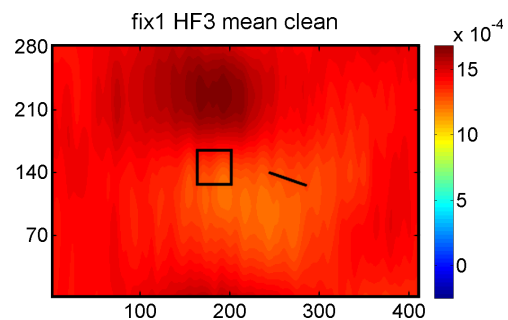


Fig. 9. Test with phantom 1 recorded at HF3 (x-y-axis: dimensions measurement area, amplitude measurement signale (digital unit))

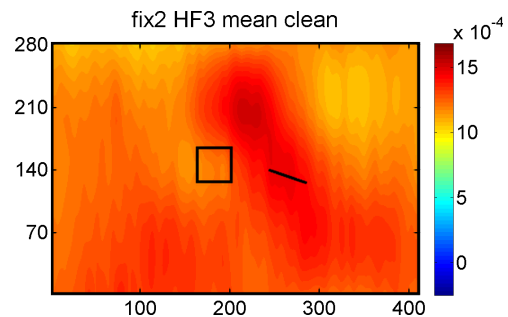


Fig. 10. Data of test with phantom 2 at HF3 (x-y-axis: dimensions measurement area, amplitude measurement signale (digital unit))

Compared to HF1 and HF2, where the orientation of the reinduced fields are within the measurement axis of the coils, the amplitude of the signals for HF3 and HF4 are smaller. This indicates again that the main measurement axis of these

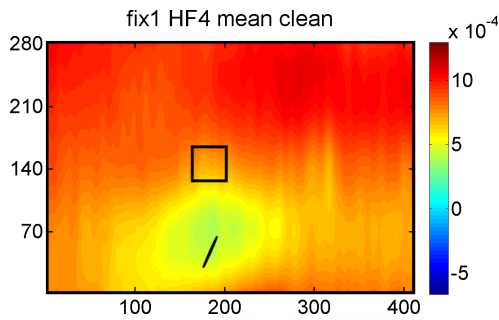


Fig. 11. Test with phantom 1 recorded at HF4 (x-y-axis: dimensions measurement area, amplitude measurement signale (digital unit))

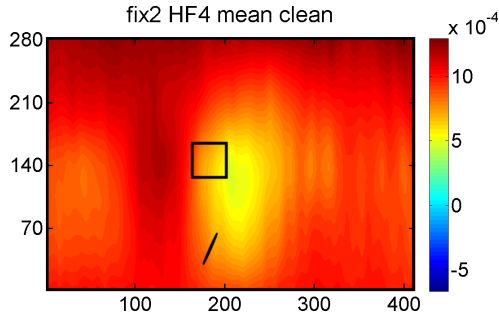


Fig. 12. Data of test with phantom 2 at HF4 (x-y-axis: dimensions measurement area, amplitude measurement signale (digital unit))

coils is between the x - and y -axis. As an example, Figure 13 shows the measurements with phantom 3. In this configuration, all coils on the test array are sensitive to reinduced fields orientated in z -direction. However, the magnitude of the recorded data is less than for fields which are orientated in the main sensitivity direction of the coils. Theoretically it is not possible to detect z -orientated components. Therefore, this must be a result of a real implementation of the array (and the used amplifier including cabling as well as the surrounding area of the array).

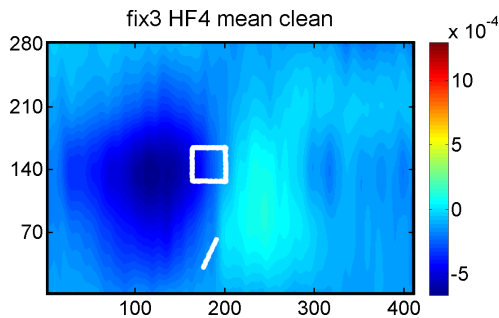


Fig. 13. Example plot for a measurement with phantom 3 (here HF4, x-y-axis: dimensions measurement area, amplitude measurement signale (digital unit))

V. CONCLUSION

In this article, a device for the characterization of magnetic induction coil arrays is presented. It was demonstrated that the measurement device can be validated with a test coil array. The ideal orientations of the sensitivity vectors of each

test coil fit to the measurement data. Areas of the coil array with measurable sensitivity, lead to high amplitudes of the measurement signal. The influences (like cables or the table under the coil array) on the coils could be detected as well (compare results with fix3). However, the device has one disadvantage. If the excitation coil generates magnetic fields which are orientated mainly in z -direction (as for the used test array), the induction of eddy currents in phantom 1 or 2 will be less than for phantom 3. This results in weaker reinduced fields. To solve this problem, new self powered phantoms will be constructed. These new phantoms will be independent of the excitation coils.

VI. ACKNOWLEDGMENTS

The authors gratefully acknowledge the German Research Foundation (DFG) for supporting this project (DFG LE 817/8-1).

REFERENCES

- [1] H. Griffiths, "Magnetic induction tomography", *Measurement Science and Technology*, Vol. 12, pp. 1126-1131, 2001
- [2] B. Karbeyaz, N. G. Gencer, "Electrical Conductivity Imaging via Contactless Measurements: An Experimental Study", *IEEE Trans Med Imaging*, Vol. 22, pp. 627-635, 2003
- [3] K. Ozkan, N. G. Gencer, "Low-Frequency Magnetic Subsurface Imaging: Reconstructing Conductivity Images of Biological Tissues via Magnetic Measurements", *IEEE Trans Med Imaging*, Vol. 28, pp. 564-570, 2009
- [4] M. Steffen, K. Heimann, N. Bernstein, S. Leonhardt, "Multichannel simultaneous magnetic induction measurement system (MUSIMITOS)", *Physiological Measurement*, Vol. 29, pp. 291-306, 2008